

# TIMERL: Efficient Deep Reinforcement Learning with Polyhedral Dependence Graphs

Pedro F. Silvestre  
Imperial College London  
p.silvestre21@imperial.ac.uk

Peter Pietzuch  
Imperial College London  
prp@imperial.ac.uk

## Abstract

Modern deep learning (DL) workloads increasingly use complex deep reinforcement learning (DRL) algorithms that generate training data within the learning loop. This results in programs with several nested loops and dynamic data dependencies between tensors. While DL systems with *eager* execution support such dynamism, they lack the optimizations and smart scheduling of *graph-based* execution. Graph-based execution, however, cannot express dynamic tensor shapes, instead requiring the use of multiple static subgraphs. Either execution model for DRL thus leads to redundant computation, reduced parallelism, and less efficient memory management.

We describe TIMERL, a system for executing dynamic DRL programs that combines the dynamism of eager execution with the whole-program optimizations and scheduling of graph-based execution. TIMERL achieves this by introducing the declarative programming model of *recurrent tensors*, which allows users to define dynamic dependencies as intuitive recurrence equations. TIMERL translates recurrent tensors into a *polyhedral dependence graph* (PDG) with dynamic dependencies as *symbolic expressions*. Through simple PDG transformations, TIMERL applies whole-program optimizations, such as automatic vectorization, incrementalization, and operator fusion. The PDG also allows for the computation of an efficient program-wide execution schedule, which decides on buffer deallocations, buffer donations, and GPU/CPU memory swapping. We show that TIMERL executes current DRL algorithms up to  $47\times$  faster than existing DRL systems, while using  $16\times$  less GPU peak memory.

## 1 Introduction

Deep reinforcement learning (DRL) extends the success of deep learning (DL) to more general settings with sequential decision-making problems [1], e.g., complex game play [2–4], robotics [5, 6], mathematics [7], algorithm design [8], and chip placement and routing [9]. DRL algorithms are also increasingly integrated in other DL workloads, including fine-tuning large language models (LLMs) using RLHF [10, 11], optimizing neural architecture search [12] or hyper-parameter

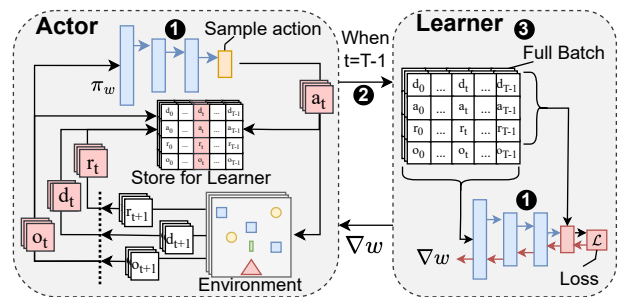


Fig. 1: Actor-learner architecture in modern DRL systems

search [13], and automated data augmentation [14].

DRL algorithms have complex computational patterns: a *learner* computes an update to a neural network from tensor data generated timestep-by-timestep by an *actor* as part of its interaction with a simulated *environment* [15] (see Fig. 1). This results in computations with nested (possibly data-dependent) control-flow, i.e., an inner loop for simulation timesteps and an outer loop for training iterations. The learner’s update computation is defined by the specific DRL algorithm, such as REINFORCE [16] or PPO [17], and it can be typically decomposed into a sum of per-timestep updates, each of which has unique *dynamic* dependencies on both past and future timesteps of the actor tensors.

Consequently, different DRL algorithms have different optimal execution strategies. Depending on how learners access the generated tensors by the actors, some algorithms may allow for parallelism between actors and learners [18], or early deallocation of tensors [19]; others may require incremental execution [20] and the offloading of large tensors to CPU memory due to limited GPU memory [21]. Conversely, when memory is not an issue, vectorization [22] can speed-up execution; and avoiding recomputation of forward activations during learning is possible for some algorithms [16, 17, 23].

Existing DL frameworks, such as PyTorch [24], TensorFlow [25], and JAX [26], struggle to support the above computational patterns and optimizations efficiently. *Eager execution engines*, such as PyTorch and TensorFlow Eager [27], adequately support dynamic control-flow and data dependen-

cies through the host language (Python). However, due to their imperative programming model, users must implement any optimizations and the execution schedule manually, based on the specific properties of an algorithm.

On the other hand, *graph-based engines*, such as TensorFlow and JAX [26], first construct a *dataflow graph*, which is then optimized automatically and scheduled for execution. Dataflow graphs, however, require statically known tensor shapes and thus cannot directly represent dynamic loop cycles, dynamic dependencies and dynamic tensor shapes. To implement DRL algorithms as a single static graph, users must (i) use complex higher-order control-flow operations [28] together with (ii) over-approximations of *loop-carried state* into static tensor shapes [29] and (iii) apply dynamic tensor slicing to extract required inputs at each timestep from the state. This is not only cumbersome for users, but it often results in excessive peak memory usage due to the over-approximation of loop-carried state. Furthermore, this is only possible when an upper bound on the number of loop iterations is known, which is not the typical case in DRL.

Current DRL systems, such as RLlib [30], CleanRL [31], and SampleFactory [32], thus inherit these limitations from the underlying DL systems. As a workaround, they entirely separate the implementation of the actor from the learner (see Fig. 1). In this *actor-learner execution* model, the actor first generates all timesteps of data before the learner computes an update as a large batch. By splitting the computation into two independent phases, the actor-learner model allows each part to be optimized as a static graph, but prevents *whole-program optimizations* and *algorithm-specific execution scheduling*, as listed above, which leads to inferior performance [33] and GPU utilization [34].

Our key insight is that, while data dependencies in DRL algorithms can be dynamic, they typically have a structure that can be represented succinctly as *symbolic expressions*, opening up a space for automatic program optimizations. We describe **TIMERL**, a new tensor execution engine for GPUs that is capable of expressing, optimizing, and scheduling DRL algorithms with dynamic data dependencies. TIMERL makes the following novel technical contributions:

**(1) Declarative programming using Recurrent Tensors (§4).** To capture the dynamic data dependencies and control-flow in DRL algorithms, we introduce *recurrent tensors* (RTs), a declarative tensor programming model inspired by recurrence equations [35].

RTs can have *symbolic* dimensions (e.g., time), which enables users to express dependencies that access past or future timesteps through *symbolic indexing*. They also handle dynamic control-flow through *branching definitions*, e.g., supporting different definitions of a tensor in different timesteps.

TIMERL’s implementation of automatic differentiation transparently accumulates over symbolic dimensions. This enables users to express DRL algorithms in terms of a single sample/iteration/timestep, which mimics pseudo-code.

**(2) Whole-program optimizations using Polyhedral Dependence Graphs (§5).** To represent the entire program as a single graph, we propose *polyhedral dependence graphs* (PDGs). Unlike a typical dataflow graph, each PDG node represents not just one execution but a dynamic set of *execution points*; edges describe how different execution points depend on each other using *symbolic expressions* obtained from the RTs.

We show that PDGs can be transformed by TIMERL to discover opportunities to *vectorize* or *incrementalize* large operations. In addition, TIMERL *fuses* dataflow-like regions of the PDG to reduce dispatching overheads and enable efficient code generation.

**(3) Execution scheduling using Polyhedral Analysis (§6).** Due to their cyclic nature, PDGs cannot be scheduled based on topological ordering. Instead, TIMERL uses polyhedral analysis [36, 37] for efficient program-wide scheduling.

By augmenting the PDG, TIMERL can automate memory management, including buffer donations, deallocations, GPU-to-CPU offloading, CPU-to-GPU pre-fetching, allowing the polyhedral scheduler to resolve when to execute them optimally. Based on this schedule, TIMERL generates a single efficient abstract syntax tree (AST) that represents the whole program. AST post-processing allows TIMERL to optimize away redundant memory-management operations and partially unroll loops to remove nested branches.

To execute programs, TIMERL specializes tensor storage methods based on access patterns, translates operations in the transformed PDG, and applies tracing code-generation [26] to fuse dataflows. It then follows the generated schedule, evaluating symbolic expressions using AST loop counters.

Our prototype implementation of TIMERL<sup>1</sup> supports multiple DL execution engines (currently PyTorch and JAX) through a simple backend interface. We evaluate TIMERL on 3 algorithms, PPO [17], traditional REINFORCE [16], and REINFORCE with  $n$ -step rewards [19], against 5 baselines.

We show that TIMERL eliminates redundant computation, parallelizes, and incrementalizes operations effectively, while performing efficient algorithm-specific scheduling. Our experiments demonstrate that TIMERL has up to  $47\times$  faster end-to-end training times than existing DRL frameworks, while remaining general and having lower peak GPU memory usage by  $16\times$ , which allows for larger scale training.

## 2 Supporting Deep Reinforcement Learning

We first introduce DRL workloads (§2.1), so that we may discuss the shortcomings of DL systems at handling their dynamic dependencies (§2.2) and how this affects downstream DRL framework design (§2.3).

### 2.1 Deep reinforcement learning

The goal in deep reinforcement learning (DRL) [1] is to learn an *acting policy*  $\pi_w$ , represented by a deep neural network

<sup>1</sup>Open-sourced post-acceptance at <https://github.com/LSDS/TimeRL>.

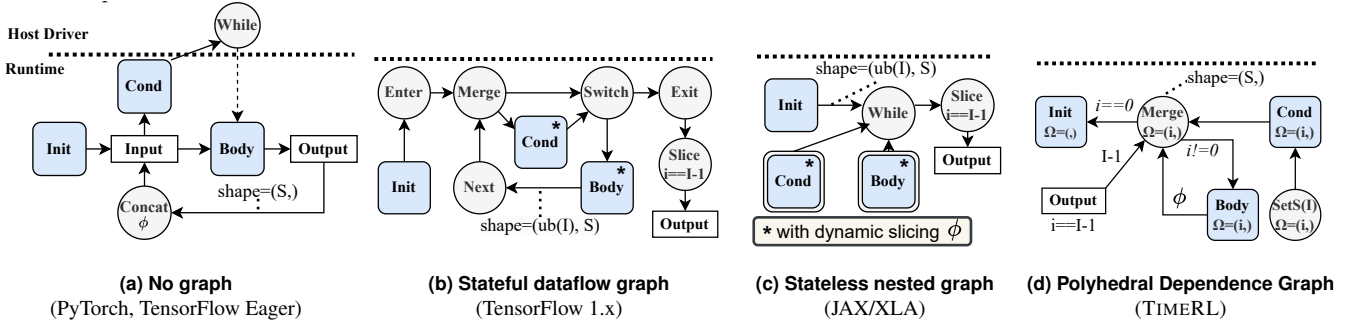


Fig. 2: Expressing dynamic data dependencies and control-flow in DL systems

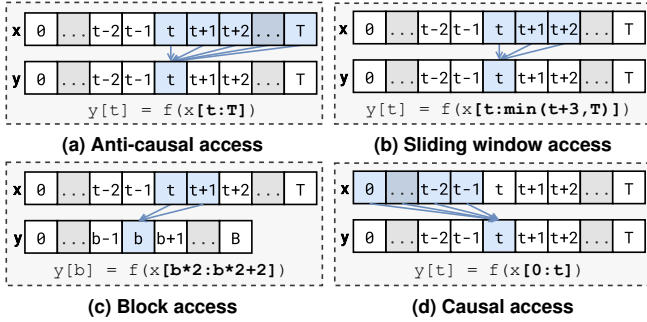


Fig. 3: DRL algorithms access past and future timesteps

(DNN) with parameters  $w$ , from *experience* data collected by sequential interactions with a simulated *environment*, as shown in Fig. 1.

At each discrete *timestep*  $t$  of the simulation, starting from the initial observation  $o_0$ , the *acting policy* produces an action  $a_t$ , which is executed in the environment and, in response, receives the next observation  $o_{t+1}$ , a done signal  $d_t$  and a reward  $r_t$ . This continues until the episode terminates at timestep  $T$ , which is either fixed or chosen dynamically. Every iteration, a *learner* computes a loss  $\mathcal{L}$  from the generated experience data, backpropagates it into a parameter update  $\nabla_w$  and uses it to update the DNN parameters  $w$ .

**Simulators.** Large-batch training helps algorithms reduce training time [38,39], de-correlate experience [23] and explore the environment [40]. Early DRL systems parallelized CPU simulators through asynchronous distribution [30, 41–43] and double-buffering [32]. However, large clusters are expensive, while asynchrony hurts data freshness and convergence guarantees [1]. CPU-based simulations underutilize GPUs [33, 34], leading to the emergence of GPU-based simulators [40, 44–47]. Thus, novel designs for synchronous and end-to-end GPU-accelerated DRL systems are needed.

**Dynamic data access.** The loss may be decomposed into a sum of per-timestep losses,  $\mathcal{L} = \sum_{t=0}^T l_t$ , in which each  $l_t$  accesses only a *portion* of the experience data dynamically, depending on the timestep  $t$ . We illustrate this in Fig. 3: Monte-Carlo algorithms such as REINFORCE [16] access all future timesteps (Fig. 3a); temporal difference methods [19] such as A2C [23] access the experience in a sliding window (Fig. 3b); PPO [17] accesses the experience in blocks (Fig. 3c).

Beyond policy-gradient methods, DQN [48] uses a backwards sliding window to stack past observations (Fig. 3b); attention mechanisms [11, 49] use causal access patterns (Fig. 3d); off-policy DRL algorithms [50] use random access patterns; SARSA [18] uses streaming access; and recurrent neural networks [51] access their own prior outputs.

Due to these fine-grained dynamic dependencies, DRL algorithms have a variety of execution strategies, which are difficult to achieve through automatic optimization and scheduling in today’s DL systems, as we explain next.

## 2.2 Dynamic computation in DL systems

Iterative dynamic computation, such as the above patterns in DRL algorithms, are difficult to represent and optimize in today’s DL systems, preventing whole-program optimizations and efficient execution scheduling. Fig. 2 shows how a dynamic data dependency  $\phi$  (e.g.,  $\phi = [i : I]$ ), in a loop over iterations  $i$ , can be expressed using control-flow in DL systems that follow the two dominant execution models: imperative and declarative (graph-based).

*Imperative* systems, such as PyTorch [24] and TensorFlow Eager [27], support dynamism well: users write imperative code that directly dispatches execution kernels to the GPU and use the control-flow statement in the host language (e.g., Python) to evaluate conditionals (Fig. 2a). These systems, however, lack a graph representation that can be optimized and scheduled automatically, thus burdening the user with writing efficient code. *Lazy eager* approaches [52] collect small subgraphs before dispatching and optimizing them, but this is still insufficient for whole-program optimization. Both eager and lazy eager approaches must perform costly movements of tensors to the CPU when evaluating conditionals as part of control-flow operations.

*Declarative (graph-based)* engines, such as TensorFlow [25] and JAX [26], first build a dataflow graph of the program before performing optimizations and execution scheduling. TensorFlow uses a flat dataflow graph with several control-flow operators [28] that encode loops and conditionals (Fig. 2b); JAX uses a single while operator [53], which nests subgraphs for loop body and condition (Fig. 2c). Both approaches, however, require static tensor shapes in the graph, and thus cannot directly express dynamic data dependencies.

As a result, users are forced into different choices on how to make the computation static, each with its own drawbacks:<sup>2</sup>

**(a) Per-shape compilation.** Users can compile a separate graph for each possible tensor shape, but this is slow for highly variable shapes [52], such as those in DRL algorithms and again breaks the program into multiple subgraphs.

**(b) Unrolling loops.** Users can fully unroll loops [26], generating all concrete instantiations of dynamic dependencies. This leads to large graph sizes that increase with the number of timesteps, increasing compilation times and losing the semantic understanding of the dynamic dependence, which prevents optimizations. It also requires a known upper bound on the number of iterations.

**(c) Over-approximation with dynamic slicing.** Users can write programs that statically over-approximate loop-carried state [29] (see Figs. 2b and 2c): they allocate a static buffer with the maximum possible size  $ub(I)$ , and modify the body and condition to use dynamic slicing to extract the inputs needed at each timestep or to write the outputs. This is cumbersome for users, requires a known upper bound on the number of iterations, and often results in excessive memory usage.

The above limitations thus impact the design of DRL frameworks, as explained next.

### 2.3 Existing DRL frameworks

DRL frameworks [30, 30, 32, 55–59] work around the above limitations by adopting the *actor-learner* execution model shown in Fig. 1. The actor-learner model splits the computation into two static graphs: (1) an *actor* graph that is executed repeatedly until termination, producing the full simulation data and storing the results in pre-allocated buffers; and, when the simulation terminates, (2) a *learner* is invoked that computes a DNN parameter update from the batch of collected experience data.

While the actor-learner model can be applied to most DRL algorithms, it has several drawbacks (indicated by the numbers in Fig. 1) due to missing whole-program optimizations:

**(1) Redundant computation.** Intermediate DNN activations produced by the actor are discarded and recomputed in the learner for use in back-propagation. This adds a substantial overhead, because it doubles the amount of DNN inference work for typical algorithms; for RNNs, the redundant work grows linearly with the sequence length.

**(2) Missed parallelism.** The execution of actors and learners must be serialized due to the coarse-grained data dependency on all data generated by the actor. This prevents parallel learning on past timesteps while acting out future timesteps, which would allow for *incremental* computation strategies. Furthermore, *online learning* algorithms are not well supported.

**(3) High peak memory usage.** The “all-at-once” learning results in high peak usage of GPU memory, potentially causing

<sup>2</sup>The following limitations also apply to eager JIT compilers [54], as they trace the dataflow graph from imperative code.

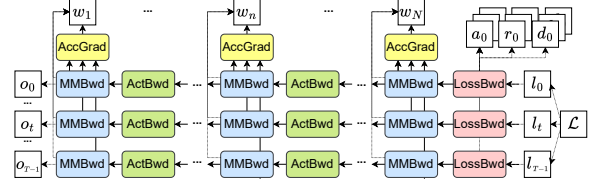


Fig. 4: Backwards graph resulting from cached actor activations

out-of-memory errors. Consider learning from  $W = H = 256$  images with  $C = 3$  color channels, at  $F = 4b$  float precision, with a batch size of  $B = 512$ , and  $T = 1,000$  timesteps—this requires  $T \times B \times (W \times H \times C \times F) / 2^{30} = 375$  GB memory to materialize the observations alone.

As a result, users often write efficient one-off implementations of specific DRL algorithms [2, 3, 31, 32, 58, 60] in eager systems (e.g., PyTorch [24]) to retain control over execution and memory management.

Users may attempt to remedy the redundant work by caching actors’ forward activations and reusing them in the backward pass for the learner. Such a manual approach, however, is less effective: due to the design of eager DL systems, a backwards graph of the full network will be created per-timestep loss  $l_t$ , as shown in Fig. 4, with each needing to be processed separately, degrading performance (§8.2). To efficiently reuse the actors forward activations, we argue that the underlying DL system must be able to *symbolically* differentiate through timesteps.

## 3 TIMERL Overview

To solve the challenges presented by dynamic data dependencies, TIMERL exploits the following key idea: dynamic dependencies can be transformed, optimized and scheduled effectively by representing them *symbolically*. Based on this idea, Fig. 5 shows TIMERL’s overall approach, which consists of four main parts:

**(1) Recurrent tensors (RTs)** allow users to express dynamic dependencies and control-flow easily as systems of recurrence equations. To achieve this, each RT has a *domain*, i.e., a set of symbolic dimensions (e.g., time, sample, sequence element), which can be indexed directly using *symbolic expressions*. This eschews the need for graph-splitting, dynamic slicing or complex control-flow operations (see §2.2). TIMERL’s implementation of *automatic differentiation* [61] propagates and accumulates gradients through symbolic dimensions as needed, producing more RTs that can be further optimized.

**(2) Polyhedral Dependence Graph (PDG).** Based on the RTs, TIMERL builds a PDG that represents the dynamic dependencies as symbolic expressions that label the edges of the graph. TIMERL optimizes the whole PDG using classical techniques, including dead and duplicate code elimination, algebraic equivalences and broadcasting removal.

To speed up execution, TIMERL employs a *vectorization* pass which finds symbolic dimensions in the domain of operations that can be executed in parallel and makes them con-

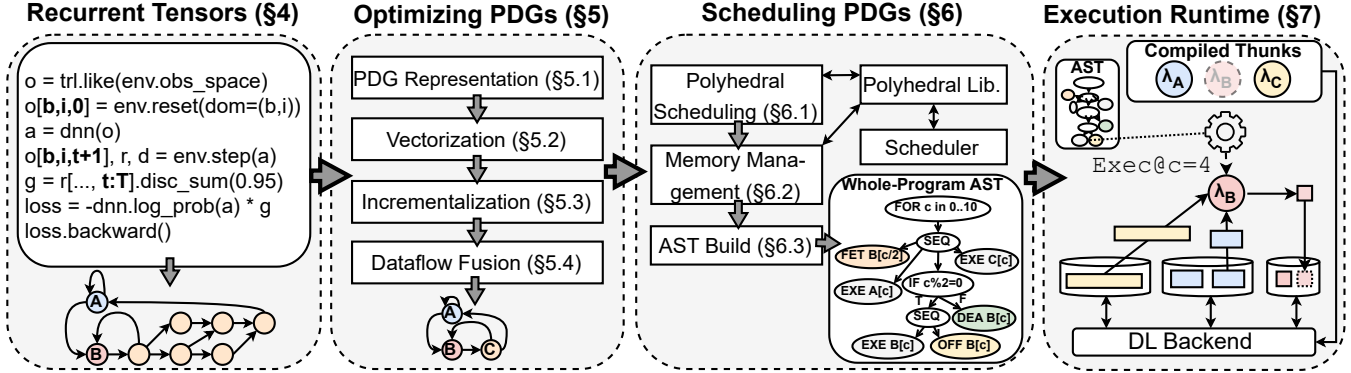


Fig. 5: Overview of how TIMERL achieves whole-program optimization, scheduling and memory management

crete. This reduces the number of symbolic dimensions and increases the amount of work done per operation invocation. To lower runtime memory requirements, TIMERL applies an *incrementalization* pass, which tiles large operations by adding symbolic dimensions that perform block accesses.

Finally, TIMERL discovers and fuses static, *dataflow-like* regions of the PDG, i.e., regions in which operations share the same symbolic dimensions and have simple *linear* dynamic dependencies. This increases performance through code generation and simplifies the scheduling problem.

**(3) Polyhedral scheduling.** RTs are declarative and thus do not prescribe an execution order. TIMERL therefore must schedule the execution of the PDG, which is non-trivial—the dynamic and cyclic dependencies prevent scheduling using simple topological sorting of the nodes.

However, PDGs are designed to enable TIMERL to adopt a *polyhedral model* [35, 36] of the computation to schedule whole computations efficiently. First, it derives a set of validity constraints, i.e., operations that must happen before others, from the PDG and solves a constrained integer linear program (ILP) using a *polyhedral scheduler* [37].

Based on the schedule, TIMERL finds opportunities for buffer reuse through *donation analysis*, which reduces memory allocations/deallocations. In addition, TIMERL augments the PDG with memory management operations, such as buffer deallocations and device/host offloading. It then uses the polyhedral scheduler to place them optimally in the schedule. Finally, it generates an abstract syntax tree (AST) from the schedule, which is post-processed for efficient execution by the execution runtime.

**(4) Execution runtime.** TIMERL’s execution runtime supports DL execution engines (currently JAX and PyTorch) as pluggable backends via a thin API. The runtime sets up physical tensor storage methods, which are specialized to how tensors are accessed, and generates code for PDG operations.

At runtime, it maintains loop counters and dynamic bounds as it interprets the AST and uses those to evaluate the symbolic dependence expressions in the PDG which describe which tensors are needed as input for operations. To efficiently execute fetch and offload instructions, the runtime employs a

combination of DLpack [62] and page-locked memory [63], as well as, pre-fetching heuristics to reduce latency.

## 4 Recurrent Tensors

Expressing the dynamic dependencies and control-flow of DRL algorithms is challenging in the programming models supported by current DL systems (see §2.2). Instead, they can be expressed naturally as *recurrence equations* [35], such as  $y[t] = f(x[t : T])$ . This is why recurrence equations are ubiquitous in algorithmic pseudocode, e.g., when defining optimizers [64], learning rate schedules [65], models [51, 66, 67], and loss functions [17, 68].

To exploit this representation, we introduce *recurrent tensors* (RTs), a declarative programming model inspired by recurrence equations. In addition to a concrete shape and datatype, an RT can be viewed as evolving over a set of *symbolic dimensions*, such as iterations,  $0 \leq i < I$ , or timesteps,  $0 \leq t < T$ , which we refer to as its *domain*.

RTs can be indexed over these symbolic dimensions using *symbolic expressions* to either express dynamic dependencies or control-flow. Symbolic expressions are a simple language, with symbols (e.g.,  $t, T, i$ ), constants (e.g., 4, False), arithmetic operations (e.g.,  $+$ ,  $/$ ,  $\%$ ), comparison operations (e.g.,  $\leq$ ,  $=$ ), boolean logic operations (e.g.,  $\&$ ,  $|$ ), and aggregations (e.g., min). To support range accesses, there is also a slice operator  $:$ , and to support RTs with multiple symbolic dimensions, there are sequence expressions  $(\cdot, \cdot)$ .

**REINFORCE with RTs.** Alg. 1 shows an example of the REINFORCE [16] algorithm using RTs. Users begin by setting up a context (line 2) with a chosen number of symbolic dimensions,<sup>3</sup> associating each dimension with a semantic meaning (line 3). Similar to PyTorch [24], DNNs are defined by composing modules, but the domain over which the network parameters vary must be stated explicitly (line 4).

The environment is then created, and the observations tensor is defined as a *branching definition* RT: the first timestep is initialized by the environment reset (line 9) and subsequent timesteps are computed by stepping the environment with the

<sup>3</sup>With zero symbolic dimensions, TIMERL behaves like a typical DL system with only concrete tensors.

**Alg. 1: REINFORCE using RTs in TIMERL**

```

1  import timerl as trl
2  ctx = trl.Context(num_dims=3)
3  with (b, B), (i, I), (t, T) as ctx:
4      dnn = trl.DNNBuilder(domain=(i,))
5          .from_env(env, hidden=[32, 32]).build()
6
7      # Acting
8      env = trl.env.make("gym.CartPole-v1")
9      o = trl.like(env.obs_space, domain=(b, i, t))
10     o[b, i, 0] = env.reset(domain=(b, i))
11     a = dnn(obs)
12     o[b, i, t+1], r, d = env.step(a)
13
14     # Learning
15     # Different access pattern -> different schedule
16     - g = r[b, i, t:T].discounted_sum(0.95)
17     + g = r[b, i, t:min(t+5, T)].discounted_sum(0.95)
18     l = -dnn.log_prob(a) * g
19     l.backward()
20     optimizer = trl.optim.Adam(dnn.params, lr=lr)
21     optimizer.step()
22
23     dnn[(i+1) % 10 == 0].checkpoint(save_path)
24     executor = ctx.compile({B: 64, I: 20, T: d})
25     executor.execute()

```

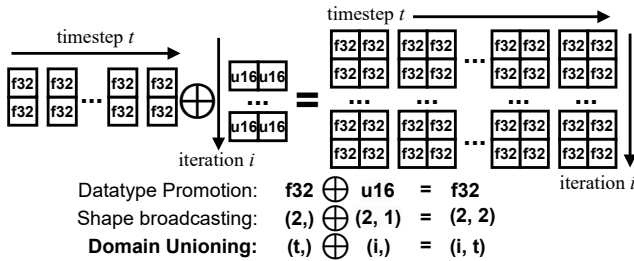


**Fig. 6: Example of automatic domain inference for RTs**

action from the DNN (line 11). The discounted rewards  $g$  of each timestep  $t$  are computed from the rewards tensor indexed by the dynamic range  $[t : T]$  (line 14), yielding a tensor with a *symbolic shape* of  $(T - t,)$ , that is then summed.

After that, the loss is computed and backpropagated (lines 16–17), and the gradients are used to update the DNN with the Adam optimizer (lines 18–19). Note how with RTs there is no need to reexecute the forward pass for learning. Expressing conditional computation, such as checkpointing (line 20), is done through *conditional indexing*, which occurs at runtime when the condition evaluates to true. Branching definitions (e.g., lines 9 and 11) are syntactic sugar over conditional indexing. Finally, the program is compiled, with the user providing either static or dynamic definitions for the symbolic dimension upper bounds (line 21).

A single line change (lines 14–15), can drastically affect the ideal execution schedule for a program (see §8.4). However, because RTs are declarative, they decouple algorithm from execution strategy, allowing users to focus only on algorithm semantics, while TIMERL handles scheduling.

**Automatic domain inference.** Annotating the domain of all RTs is unnecessary, because TIMERL infers the domain of most RTs from the domain of sources. For example, symbolically indexing an RT with a constant (e.g., 5 or  $T$ ) on a symbolic dimension  $d$  removes  $d$  from its domain. When two RTs interact, their domains are automatically unioned (similar to shape broadcasting or datatype promotion), as shown in Fig. 6. In this example, the left RT varies with timesteps  $t$ , while the right RT varies with iterations  $i$ . Their interaction produces an RT which varies with both symbolic dimensions (i.e., has a domain of  $(i, t)$ ).

If an RT is not explicitly symbolically indexed ( $g$  in line 16), it is treated as if indexed *linearly* (i.e.,  $g[b, i, t]$ ), making it behave like a standard tensor in the common case. In TIMERL, every aspect of computation is defined using RTs, including the optimizer (e.g., Adam [64]), simulation environments [15], and replay buffers [69]. Automatic domain inference therefore allows, e.g., for learning rate schedules, to be easily expressed as RTs too, e.g.,  $lr[i] = lr[i - 1] \times 0.98$ , and be integrated with the optimizer without code changes due to domain inference.

## 5 Polyhedral Dependence Graphs

TIMERL uses RTs to construct a whole-program *polyhedral dependence graph* (PDG), which encodes dynamic dependencies. Below, we describe the PDG abstraction in detail and explain how it supports symbolic backpropagation (§5.1). After PDG construction, TIMERL applies typical compiler optimizations to the PDG, such as dead and duplicate code elimination, algebraic equivalences, and broadcasting removal. We focus on three key transformations: vectorization (§5.2), incrementalization (§5.3), and dataflow fusion (§5.4).

### 5.1 PDG representation

A PDG is a directed multigraph of operations, in which each operation can have multiple input and output tensors. Cycles (even self-loops) are allowed.

Each *operation*  $o$  is tagged with a domain  $\Omega(o)$ , which is the set of integer points in  $\mathbb{Z}^n$  at which the operation must be evaluated; each *edge*  $o_1 \xrightarrow{iid, \phi, \psi, oid} o_2$  is annotated with the sink input identifier *iid*; a symbolic *dependence expression*  $\phi$ ; an optional *condition*  $\psi$  and the source output identifier *oid*. It indicates that  $o_1$  (the sink) at point  $p \in \Omega(o_1)$  *depends on* output *oid* of  $o_2$  (the source) at points  $\phi(p)$  when  $\psi(p)$  is True. The domain  $\Omega$ , dependence expressions  $\phi$ , and conditions  $\psi$  come directly from the domains and symbolic expressions of the RTs that defined them (see §4).<sup>4</sup>

**Tensor operations.** The operations within the PDG come from a minimal set of 40 stateless operators, most of which are typical elementwise maps, reductions, scans, layout or indexing operations. Layout operators (e.g., ReshapeOp, SliceOp) can hold symbolic shapes and indexes in their parameters.

<sup>4</sup>In the remainder of the paper, we treat operations as having a single input and output to simplify notation; in figures, we also omit *linear* dependencies (i.e., maps  $i$  to  $i$ ,  $t$  to  $t$ ).

In addition, a few new operators are required for dynamic computation: MergeOps are needed to support RTs with branching definitions. They conditionally select which input to copy to their single output based on edge conditions  $\psi$ ; EvalSymbolOps inject the runtime value of a symbol (e.g., the current timestep  $t$ ) into the execution; SetSymbolOps inform the runtime of when the value of a dynamic upper bound is found. Users do not have direct access to these operators, because they are automatically inserted by the compiler. Finally, UDFOps allow users to register custom operations, which may access *external state*. They are used by TIMERL to integrate with environments [15] and replay buffers [69, 70].

**Symbolic backpropagation.** When backward() is called on an RT, typical automatic differentiation [61] is used to compute the input gradients given the output gradients. A challenge, however, is that TIMERL must also propagate or accumulate gradients through symbolic dimensions. Thus, for a given RT  $y[p] = f(x[\phi(p)])$ , the gradient of  $x$  is an RT with the same shape, datatype, and domain,

$$\nabla x[p'] = \sum_{p \in \phi^{-1}(p')} f'(\nabla y[p]),$$

where  $f'$  is the derivative of the operation  $f$  and  $\phi^{-1}$  is the *inverse* of the dependence relation. Intuitively, inverting a dependence expression converts “what source points does the sink point  $p$  depend on?” to “what sink points depend on source point  $p$ ?”. For example,  $[t + 3]$  inverts into  $[t - 3]$ ,  $[t : T]$  into  $[0 : t + 1]$ , and  $[0 : T]$  into  $[0 : T]$ . Since a single point of  $x$  may contribute to several points of  $y$ , the gradient of  $x[p']$  must sum the gradient contributions from all  $y$  points it contributed to. When backpropagating through a conditional branch (MergeOp), the gradient must only flow to the input from which the output was computed. Thus, the chain-rule for a MergeOp produces other MergeOps with the same conditions, which conditionally copy from the output gradient or zeros.

We present a small PDG in Fig. 7a that computes in a MergeOp the timestep-wise sum of a MulOp’s output. At  $t = 0$ , the sum is the MulOp’s output at  $t = 0$ ; at each subsequent step  $t$ , the sum adds the current MulOp output to the previous step’s MergeOp result. Though correct, this incremental PDG is inefficient. We will now show how it can be progressively transformed (Fig. 7b) into a more efficient equivalent form.

## 5.2 Vectorization

The *vectorization transformation* reduces the execution time of PDGs by moving dimensions from symbolic to concrete. This creates fewer and larger parallel executions, at the cost of increased memory usage. The first step of vectorization is to find incremental scans, reductions and stencils implemented using MergeOps and dynamic indexing, and to *lift* **A** them through simple pattern-matching into batch operations such as SumOp, CumSumOp and ConvOp.

Then, Alg. 2 is used to *vectorize* **B** all other operations by applying it to each symbolic dimension  $d$ . The algorithm first

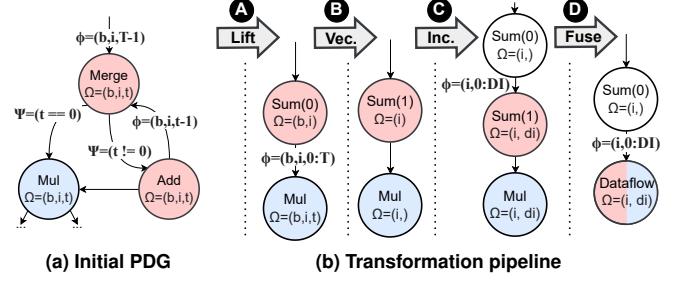


Fig. 7: Evolution of a PDG through the transformation pipeline

### Alg. 2: VECTORIZE transformation

```

Input: G (PDG), d (Symbol), D (Symbol)
1 foreach op in GetVectorizableOps(G, dim) do
2   | G.AddOp(VectorizationRule(op))
3 foreach (snk, src, φ) in G.Edges() do
4   | idx ← Ω(src).GetIndex(d)
5   | vsnk, vsrc ← GetVectorizedOpOrNone(snk, src)
6   | if vsnk and vsrc then
7     | φ ← φ.DropAtIndex(idx)
8   | else if not vsnk and vsrc then
9     | vsrc ← G.AddIndexSelect(vsrc, idx=d)
10  | else if vsnk and not vsrc then
11  |   | if d ∈ Ω(src) then
12  |     | φ ← φ.ReplaceAtIndex(idx, 0:D)
13  |   | else
14  |     | vsrc ← G.AddExpand(src, (D, src.shape))
15  |   G.ReplaceEdge(vsnk, vsrc, φ)

```

finds all vectorizable operations, applies a *vectorization rule* to each (lines 1–2), and then updates the edges to reflect the changes (lines 3–15).

Depending on whether one, both, or neither of the source and sink of an edge are vectorized, a different transformation is applied to the connecting edge. When both are vectorized (line 6), the indexing of dimension  $d$  is dropped from the dependence expression  $\phi$  (line 7). When the sink is not vectorized and the source is, the sink must use an IndexSelectOp to extract the correct  $d$ -th element of the source at each step  $d$  (lines 8–9). When the sink is vectorized and the source is not, if the source varies with  $d$ , the sink should now take as input all values of the source at each step  $d$  (lines 11–12). If the source does not vary with  $d$ , the source value must be expanded to the size  $D$  that the sink expects (lines 13–14).

The vectorization rules themselves are simple: elementwise operations are not modified, while operations with a dimension parameter (e.g., SumOp, SqueezeOp) have it incremented; operations with shapes (e.g., ReshapeOp) have the vectorized dimension’s upper bound  $D$  prepended to the shape parameter.

Clearly, only operations with  $d$  in their domain can be vectorized over  $d$ . However, due to the cyclic nature of PDGs, it is challenging to decide what operations can be vectorized over  $d$  while avoiding an *unschedulable* PDG with impossible cycles. To avoid this, TIMERL applies the following conservative approach: we define a cycle as *trivial* on  $d$  if all symbolic indexes of that dimension are  $[d]$  itself or a constant expression (e.g.,  $[0 : D]$ ,  $[5]$ ,  $[0 : 5]$ ). Operations in non-trivial

**Alg. 3: INCREMENTALIZE transformation**


---

**Input:**  $G$  (PDG),  $o$  (Op),  $bs$  (int),  $di$  and  $DI$  (Symbol)

```

1 fun Incrementalize( $G, o, bs, di$ ):
2   IncRecursive( $G, o, o.dim, bs, di$ )
3   UpdateEdges( $G, di$ )
4   block_reduction  $\leftarrow$  ReduceOp( $G, o, 0:DI$ )
5    $G.MoveDependents(o, block\_reduction)$ 
6 fun IncRecursive( $G, o, i, bs, di$ ):
7    $G.InsertOp(IncRule(o, i, bs, di))$ 
8   if  $o$  is PermuteOp then
9      $i \leftarrow o.permutation.GetIndex(i)$ 
10  else if  $o$  is SqueezeOp and  $o.dim \leq i$  then
11     $i \leftarrow i + 1$ 
12  else if  $o$  is UnsqueezeOp and  $o.dim > i$  then
13     $i \leftarrow i - 1$ 
14  if  $o$  is ExpandOp and  $o.dim == i$  then
15    return
16  foreach ( $o_d, \phi$ ) in  $G.Dependencies(o)$  do
17     $s \leftarrow \phi.NumSlices()$ 
18    if  $s < i$  and  $G.Mem(o_d) > MAX\_MEM$  then
19      IncRecursive( $G, o_d, i + s, bs, di$ )

```

---

cycles cannot be vectorized. Operations in trivial cycles must all be vectorized simultaneously or none can be.

### 5.3 Incrementalization

Some operations may demand too much memory, especially after vectorization. To address this, TIMERL then *incrementalizes*  $\textcircled{C}$  the PDG using Alg. 3: it breaks-up large operations into smaller blocks of size  $bs$  by adding a new symbolic dimension  $di$  to the domain of operators. The block size is chosen so the memory requirements of operations remain below a threshold. This transformation allows TIMERL to implement *gradient accumulation* [20] transparently.

Since reductions (e.g., SumOp, MaxOp) reduce a specific concrete dimension ( $i = o.dim$ ), they are a natural starting point for incrementalization. Given a large reduction operation  $o$ , Alg. 3 incrementalizes  $o$  and each of its dependencies  $o_d$  recursively (line 2). It then updates the affected PDG edges (line 3), and reduces the results over all blocks  $0 : DI$  (line 4) before moving all dependents of  $o$  to this new reduction (line 5). Each recursive step (line 6) also tracks the index  $i$  of the concrete dimension being incrementalized, as it changes due to layout operations (lines 8–13). It stops the recursion when it finds either an ExpandOp that creates the dimension (line 14), or a dependency that is not vectorized or has a memory requirement below the threshold (lines 16–18).

### 5.4 Fusion

A PDG often contains *regions* with only *linear* dependencies and the same domain for all operations. Inside these regions, the PDG behaves as a dataflow graph, directly passing the outputs of one operation to the inputs of another. The goal of the *fusion transformation* is to find and *fuse*  $\textcircled{D}$  these regions into a single DataFlowOp operation. This not only enables efficient code-generation by DL compilers [26, 54, 71], but also lowers the runtime dispatching overhead and simplifies the scheduling problem.

The fusion algorithm first finds these groups by assigning each operation a unique group identifier, and then merges neighbouring groups that have the same domain and only linear edges between them. Constants and layout operations with smaller domains can also be grouped into groups with larger domains. This is iterated until convergence.

TIMERL then replaces each group with a new DataFlowOp operation, and updates the edges to reflect this. Dynamic operations (e.g., RNGOp, UDFOp, MergeOp) are excluded from fusion since they cannot be statically compiled.

## 6 Polyhedral Scheduling of PDGs

RTs are declarative and thus do not prescribe an execution order. We show how a *polyhedral model* [36, 37] can address this challenge while enabling algorithm-specific scheduling. Scheduling occurs in two rounds: (1) TIMERL first finds an execution schedule (§6.1), freezes it, and then (2) uses it to schedule memory management operations (§6.2).

### 6.1 Polyhedral execution scheduling

Scheduling DRL programs is challenging due to their dynamic, cyclic dependencies. The polyhedral model [36, 37], originally developed for scheduling uniform recurrence equations [35], has since evolved to support much more complex computations [72]. However, today it is primarily used to optimize small loop nests in imperative programs [73, 74], as modeling arbitrary programs in it remains difficult [75].

In a polyhedral model, each tensor  $x$  has its *domain* represented by a polyhedron,  $\Omega_x = \{p \in \mathbb{Z}^n \mid \text{constraints}\}$ , which is the set of integer points in an  $n$ -dimensional space that satisfy a set of *inequality constraints*. A dependence of tensor  $x$  on  $y$  is also represented by a polyhedron in the product of the two domains,  $\phi_{x \rightarrow y} = \{(p, p') \in \Omega_x \times \Omega_y \mid \text{constraints}\}$ . For simplicity, we treat  $\phi_{x \rightarrow y}$  as a function  $\phi_{x \rightarrow y}(p) = \{p' \in \Omega_y \mid (p, p') \in \phi_{x \rightarrow y}\}$  that, given a point in  $\Omega_x$ , yields all points in  $\Omega_y$  that it depends on.

Scheduling in a polyhedral model finds a *schedule function*  $\theta$  that maps each point of the domain of tensors to an *execution time* in a larger space  $\mathbb{Z}^s$ ,  $s > n$ , and where the lexicographic order determines what operation executes first. A valid schedule must respect all dependencies, i.e.,  $\forall \phi_{x \rightarrow y}. \forall p_x \in \Omega_x. \theta(\phi_{x \rightarrow y}(p_x)) \prec \theta(p_x)$ , where  $\prec$  is the lexicographic smaller-than comparison. Finding schedules thus involves solving a complex integer linear program (ILP) [36], which is constrained by the dependencies in the computation.

PDGs are not arbitrary unconstrained programs. Extracted from RTs, PDGs already represent tensor domains, dependencies and conditions explicitly using symbolic expressions. Thus, TIMERL can directly create domain and dependence polyhedra from the PDG, allowing us to leverage the polyhedral model for whole-program scheduling. Furthermore, because we have fused large dataflow regions, the number of operations is reduced, making the ILP more tractable even for large programs.



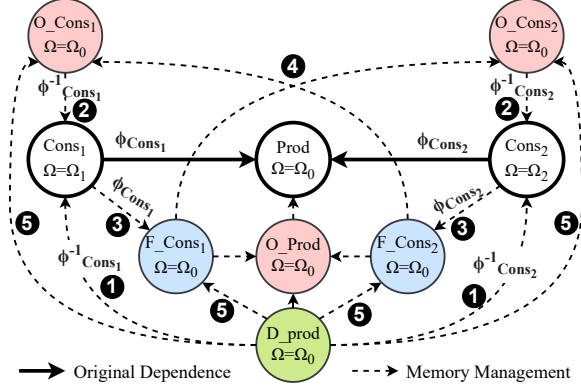


Fig. 8: TIMERL augments a PDG for memory management

The challenge is in translation. Polyhedral schedulers require polyhedra to be expressed using Presburger formulas [76], which are similar to our symbolic expressions (see §4), but do not support range  $:$ , modulo  $\%$ , max or min operators. Instead, presburger formulas use quantifiers ( $\forall, \exists$ ), which still enable us to express the full complement of symbolic expressions. For example, a slice  $[a : b]$  can be expressed as  $\forall x \in \mathbb{Z}. a \leq x < b$ .

TIMERL additionally produces a set of *proximity constraints* which, for example, consider only the upper bound of slice expressions and ignore constant arguments in min/max expressions. These constraints guide the scheduler towards efficient schedules with more parallelism and reuse of recently computed tensors, resident at higher levels of the GPU memory hierarchy. TIMERL thus solves the ILP and stores the resulting schedule function  $\theta$  for scheduling memory management operations, as discussed next.

## 6.2 Memory management

The current execution schedule would allocate memory but never release it, leading to out-of-memory errors. To address this, TIMERL also schedules memory management operations: (i) donations, (ii) deallocations and (iii) swapping (i.e., offloading to CPU memory and fetching from GPU memory).

**Finding buffer donations.** Given the PDG’s stateless nature, it is important to detect when a tensor will be deallocated, and thus its backing memory buffer can be *donated* to be reused by another operation. For example, DNN parameters, which are represented as a cycle in the PDG between a MergeOp and the optimizer should reuse the same buffers. Given a schedule  $\theta$ , the last user  $o^u$  of tensor  $o^d$  is the tensor that, for every point  $p$  in the domain of  $o^d$ ,  $o^u$  accesses  $p$  *after* every other competing dependent  $o^c$ . Formally,

$$\exists o^l \in \text{Dependents}(o^d). \forall o^c \in \text{Dependents}(o^d). \forall p \in \Omega(o^d). \\ \theta(\phi_{o^c \rightarrow o^d}^{-1}(p)) < \theta(\phi_{o^l \rightarrow o^d}^{-1}(p))$$

**Scheduling deallocations and swap.** Scheduling deallocation and swapping operations further requires careful ordering of operations in relation to each other and executions. Given

the complexity of manual analysis, TIMERL instead carefully augments the PDG with extra memory management operations and dependencies, and then leverages the polyhedral scheduler to find the correct schedule.

Fig. 8 gives an example with three tensor operations: Prod produces a tensor that Cons<sub>1</sub> and Cons<sub>2</sub> consume. We focus on the memory management operations for Prod. Memory management operations, such as deallocations (green), device-to-host offloads (red) and host-to-device fetches (blue), must apply to every point in the domain of the tensor they manage,  $\Omega(\text{prod})$ , and thus must share this domain.

The deallocation of each  $\text{Prod}[p]$  must happen only once all consumers have finished using it. The consumer points that depend on  $p$  are found by inverting the dependence expression from the consumer to the producer. This is then used to add a dependence from the deallocation to the consumer (1 in Fig. 8), ensuring the deallocation waits for the consumers.

To support swapping, TIMERL inserts an offload-fetch pair for every consumer of a tensor, plus an initial offload after production. Similar to deallocations, the offload of a point must happen *after* the consumers are done using it (2). The fetches, on the other hand, must happen *before* the use of the points by consumers—this is represented by another dependency added by TIMERL (3). To ensure schedules that combine fetches and offloads from different consumers remain invalid, TIMERL adds linear dependencies between fetches and offloads created from different consumers based on which one executes first (4). Finally, since the deallocation must happen after all other fetches and offloads, TIMERL adds linear dependencies between all (5).

To prevent excessive swapping, TIMERL only swaps tensors that have more than one symbolic dimension (always needed in-memory), and it does not swap tensors with size below a configurable threshold. By augmenting the PDG in this way, TIMERL eschews the need for complex manual analysis and can automatically find an efficient memory management schedule for any program.

## 6.3 Abstract syntax tree generation

The schedule function  $\theta$  output by the polyhedral scheduler [37] is not directly executable. It must be transformed first into an abstract syntax tree (AST). Using the polyhedral library [36], TIMERL thus traverses this representation [77] and emits an equivalent AST in our own format:

- **Loop:** a generic loop with a counter symbol, start, end, step, condition and body sub-AST;
- **If:** a conditional with then and else sub-ASTs;
- **Sequence:** a block of AST nodes executed in order;
- **Execute:** executes operation  $o$  for point  $p$  given by a mapping from AST counters to domain symbols; and
- **Deallocate/Fetch/Offload:** execute the instruction for points  $P$  given by a mapping from AST counters to domain symbols of the producer.

To generate efficient ASTs, TIMERL applies further optimizations: (1) it *partially unrolls* loops such that the number of Ifs inside loops is minimized; (2) it *promotes* static loops that contain only memory management operations into batched instructions by mapping the loop’s range to a slice of points; and (3) it finds and removes redundant fetches and offloads by (i) removing any offload followed by a fetch or deallocation for the same tensor and covering a *superset* of the original set of points; and (ii) removing fetches for already in-memory tensors.

## 7 Execution Runtime Implementation

The prototype implementation of TIMERL is written in ~25,000 lines of Python code. Our runtime (rightmost block of Fig. 5) is responsible for taking the PDG, AST, and the user-provided DL backend, and executing the program.

**Tensor storage.** Tensors in the PDG have varied access patterns, requiring tailored storage strategies at runtime. TIMERL currently has two tensor storage implementations: (1) a *point store* is a simple map from a tuple of integer indices (runtime symbol values) to runtime tensors, which makes point insertion, access and removal fast at the cost of requiring concatenation for slice accesses; and (2) a *block store* is a map from a tuple of indices to large pre-allocated runtime tensors, which are aligned when possible to the access expressions in the PDG. This allows for fast slice accesses, but requires fast in-place mutation of tensors and can delay memory management requests (deallocation and offloading).

TIMERL determines the type of storage used by examining accesses in the PDG before scheduling. Tensors that are only point-accessed are stored in a point store, while tensors that are slice-accessed are stored in a block store. The block size is determined by the largest slice access to the tensor.

**Backends** must implement a thin backend interface, which has methods for (i) allocating and deallocating tensors, (ii) moving tensors between devices, and (iii) executing specific tensor operations (dynamic update and stack) required to implement the tensor stores. Each backend must also implement DLpack [62] zero-copy conversion to connect with other DL frameworks and GPU-based simulators with minimal data copying. The tracing-based compilation implementation of a backend is used to generate executable *thunks* for DataflowOp operations.

**Thunk launchers** evaluate a thunk’s input dependence expressions at the current execution point  $p$  using the runtime AST loop counters, in order to index tensor stores. They then execute the thunk with the retrieved tensors and store the outputs back in tensor stores at point  $p$ .

**Buffer management.** JAX [26], as a TIMERL backend, lacks page-locked memory and thus cannot perform asynchronous host-to-device transfers. Asynchronous fetch/offload is essential for high GPU utilization [21], but, without page-locked buffers, the CPU has the overhead of first copying tensors syn-

chronously [63]. To address this, TIMERL uses a *page-locked buffer manager* that zero-copies tensors from any backend to CUDA arrays via DLpack, and directly transfers them into page-locked memory.

## 8 Evaluation

We evaluate TIMERL to answer the following questions: Do TIMERL’s abstractions and optimizations lead to more efficient computation compared to existing approaches? (§8.2) Does TIMERL’s memory management enable larger scale DRL training? (§8.3) Can TIMERL effectively support algorithm-specific execution schedules? (§8.4)

### 8.1 Methodology

We evaluate TIMERL on (a) PPO [17] (one epoch per iteration), (b) REINFORCE [16] and (c) REINFORCE with  $n$ -step returns [19]. We run TIMERL with its JAX and Torch backends, and compare against three representative DRL implementation types: (i) synchronous performance-focused frameworks (SampleFactory v2.1.1 [32], RLGames v1.6.1 [58]), (ii) single-file algorithm implementations (CleanRL commit e648ee2 [31]), and (iii) scalable distributed DRL frameworks (Ray RLlib v2.5.0 [30]).

To focus on execution overheads, we employ a single GPU-accelerated test environment [40, 45], except for RLlib which lacks GPU environment support. Each experiment runs twice, once with default allocators for end-to-end performance, and once without caching allocators to measure true memory usage, discarding the first iteration to ensure warm-up.

All experiments use the same hardware and software configuration. We use a server with an AMD EPYC 7402P 24-core CPU, 384 GB of DDR4 RAM (3200 MT/s) with an NVIDIA RTX A6000 GPU (48 GB of GDDR6 RAM, PCIe Gen4  $\times$  16 at 32 GB/s). We run Ubuntu v22.04 with Linux kernel v5.15, CUDA v12.1, PyTorch v2.5.1, and JAX v0.4.35.

### 8.2 Training performance for PPO

We evaluate the end-to-end training performance of TIMERL with PPO, a popular DRL algorithm with an anti-causal dependency (r[t:T]) that prevents parallel acting and learning. We start with a default configuration with an episode length of 250, 512 environments, 64 parameters per layer, 2 hidden layers, and a  $3 \times 4 \times 4$  observation shape, and we then vary each parameter individually.

Fig. 9 shows the result by reporting iteration time and GPU utilization. TIMERL (TRL), using both its JAX and Torch backends, has consistently lower iteration times than all other baselines. TIMERL is up to  $47 \times$  faster than RLlib, and on average  $2.18 \times$  faster than the next fastest system, CleanRL, which is a hand-coded PPO implementation. There are several reasons for this: TIMERL’s PDG representation supports holistic optimizations, such as deduplicating the forward passes and caching activations. In addition, TIMERL’s automatic vectorization, efficient scheduling and code-generation of fused dataflow regions further improve performance.

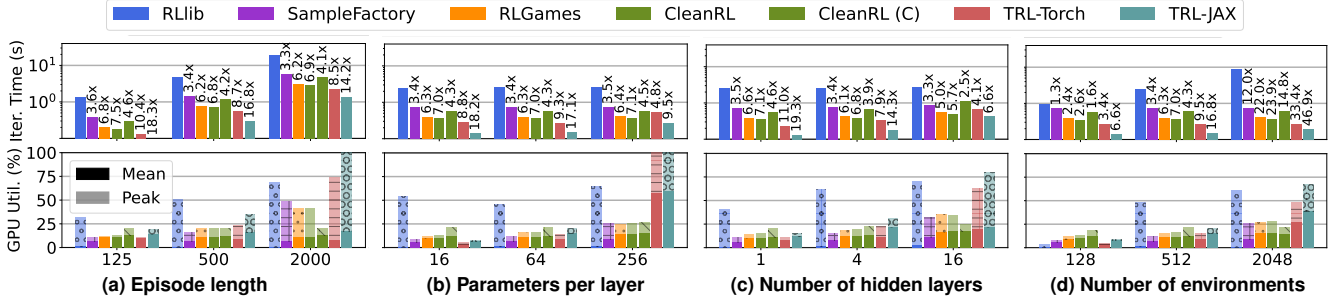


Fig. 9: End-to-end iteration time and GPU utilization for PPO at small-to-medium scale.

TIMERL’s Torch backend is consistently slower than the JAX backend. We attribute this to a bug<sup>5</sup> in Torch’s graph capture system [54], preventing us from using the newer `torch.compile` for DataflowOp code-generation. Therefore, we rely on the older `torch.jit.trace` API, which lacks Triton’s profile-guided optimization [71] and CUDAGraphs [78] to reduce kernel launch overhead, both of which JAX uses.

As episode length grows (Fig. 9a), all systems slow linearly, narrowing relative performance differences slightly. Adjusting the number of parameters per layer (Fig. 9b) does not affect relative performance until 256 parameters, where TIMERL begins incrementalizing the backward pass. Increasing hidden layers (Fig. 9c) slows down all systems, but particularly TIMERL, likely due to Python-level AST interpretation overheads that in future work may be resolved by code-generating efficient C++ AST executors. Running more environments simultaneously (Fig. 9d), however, improves TIMERL’s relative performance due to several factors: (i) unlike RLlib, TIMERL supports GPU-accelerated environments; (ii) interpretation overheads are amortized by batch size; and (iii) activation caching becomes more impactful.

At this scale, the GPU is generally underutilized by all systems. However, TIMERL’s GPU utilization is on average higher than the other systems, which indicates efficient use of the hardware due to our optimizations. Peak utilization is also high for RLlib, but this is due to the large CPU-GPU data transfer performed every iteration. Interestingly however, when increasing parameters per layer (Fig. 9b), TIMERL’s utilization grows far more than the other systems. This may indicate that despite being faster already, TIMERL may be missing some algebraic simplifications that the other systems are performing, leaving room for future improvement.

We modify CleanRL to cache and reuse forward activations in the same way as TIMERL. Fig. 9 shows that the end-to-end iteration time of CleanRL is on average 70% slower when caching (CleanRL (C)) is enabled. As explained in Section 2.3 such a strategy cannot be implemented efficiently in modern DL systems because each timestep creates its own backpropagation graph (Fig. 4). On the other hand, TIMERL’s symbolic automatic differentiation creates a single backpropagation graph with a symbolic time dimension.

<sup>5</sup><https://github.com/pytorch/pytorch/issues/134616>

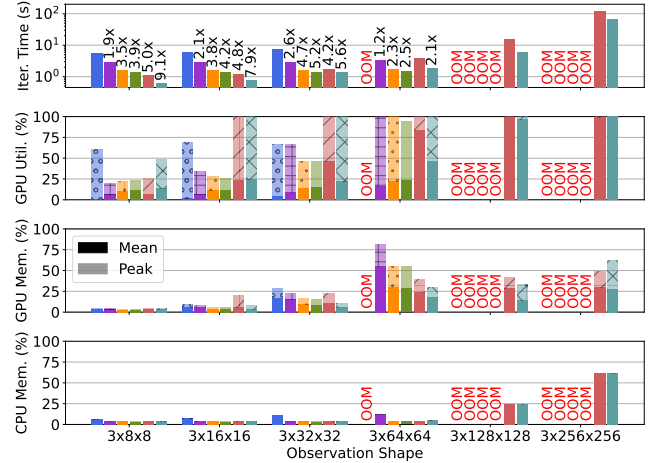


Fig. 10: Scaling to large observation sizes with PPO

### 8.3 Memory management

Training DRL models from image observations is a common use-case in robotics [79], autonomous driving [80] and health-care [81], that actor-learner DRL frameworks struggle with. Image resolutions impact both model task performance and system memory usage, as larger images require more memory to store and process. In this experiment, we halve the number of environments to 256, but quadruple the episode length to 1,000 and show iteration times, GPU utilization and memory, and CPU memory, as we scale observations up to  $3 \times 256 \times 256$ .

As Fig. 10 shows, independent of the algorithm, the actor-learner approach stores and learns from all observations at once, resulting in a GPU peak memory usage that exceeds capacity. RLlib enters a fail-retry loop before  $3 \times 64 \times 64$ , while the other baselines fail to scale past it, due to out-of-memory (OOM) errors. In contrast, TIMERL scales to  $3 \times 256 \times 256$  ( $16 \times$  larger) while balancing GPU memory with CPU memory usage, through automatic incrementalization and swapping (see §5.3 and §6.2). TIMERL uses incrementalization after  $3 \times 32 \times 32$ , leading to a slight slow-down, and swapping is used after  $3 \times 128 \times 128$ . To scale PPO further, TIMERL would require more CPU memory, which easier to add than GPU memory.

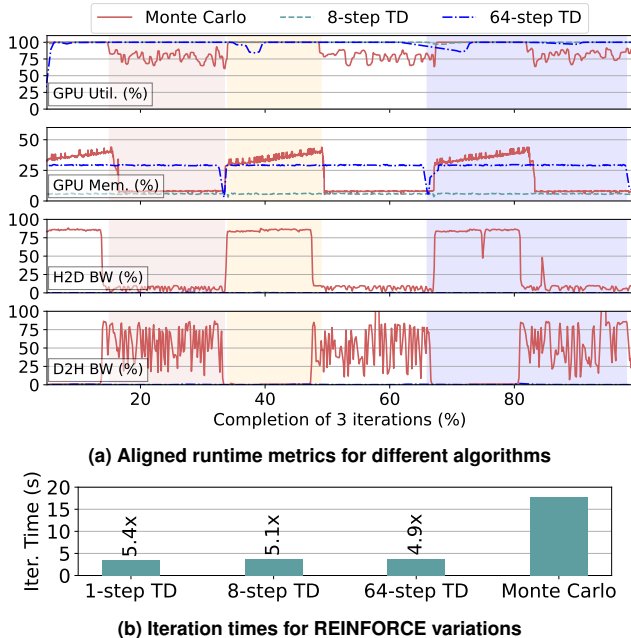


Fig. 11: Algorithm-specific scheduling with TIMERL-JAX

#### 8.4 Algorithm-specific scheduling

We explore TIMERL’s ability to adapt scheduling to specific properties of the DRL algorithm in the  $3 \times 256 \times 256$  observations setting. We use the two variations of REINFORCE shown in Alg. 1, which use: (i) traditional Monte Carlo [16] returns; and (ii)  $n$ -step temporal-difference (TD) returns [19]. Despite the one line difference, Fig. 11a shows how TIMERL executes the two algorithms differently.

Since Monte Carlo (red line) uses an anti-causal access pattern ( $r[t : T]$ ), TIMERL must wait until the simulation finishes before learning. During simulation (red shading), TIMERL continually offloads observations to CPU memory, maintaining low memory usage, but not fully utilizing the GPU. Once finished, learning begins (orange shading), and TIMERL incrementally swaps observations back to GPU memory, learning from them while fully utilizing the GPU.

With  $n$ -step TD (blue and teal lines), however, TIMERL can execute a different strategy due to the window access pattern ( $r[t : \min(t + n, T)]$ ): after an  $n$ -step delay, it begins computing gradients *in parallel* with simulation (blue shading). This enables TIMERL to: (i) fully utilize the GPU through parallelism; (ii) only store the last  $n$  observations, deallocating older data as early as possible; and (iii) avoid swapping due to the lower memory demand. Due to the  $n$ -step delay before parallel learning, 64-step TD still experiences a slight GPU utilization dip, which 8-step TD does not.

For smaller  $n$ , TIMERL is able to parallelize work earlier, leading to faster iteration times, as shown in Fig. 11b. In either case, TIMERL uses the most effective execution schedule for each algorithm, maintaining low peak GPU memory usage even with  $3 \times 256 \times 256$  observations, allowing for large-scale training even on a single GPU.

## 9 Related Work

**Polyhedral frameworks in DL.** Tensor Comprehensions [74] optimizes tensor computations through polyhedral loop fusions, tilings and parallelization. PPCG [82] is C-to-CUDA compiler that performs similar loop optimizations and additionally manages GPU memory across the hierarchy. TVM [83] and Triton [71] are similar DL compilers that do away with direct polyhedral modeling. In general, these works perform low-level optimizations on specific loop nests, while TIMERL uses the polyhedral model to schedule the high-level execution of complete DRL programs.

**Memory management in DL.** Prior work has explored gradient accumulation [84] and swapping [21, 85] to reduce memory pressure. TIMERL transparently integrates these ideas at a program level automatically through transformations (incrementalization) and scheduling (fetches and offloads). Recomputation [86, 87] deallocates and recomputes intermediate activations to reduce memory usage. TIMERL does not currently support automatic recomputation.

**Dynamic DL systems.** FractalTensor [88] introduces a tensor abstraction similar to recurrent tensors, but focuses on memory reuse and fine-grained parallelism optimization, unlike TIMERL’s emphasis on whole-program optimization. JANUS [89] and PyTorch 2 [54] have some support for dynamic computation compilation through a combination of symbolic shapes, speculative compilation, and runtime assertions that trigger recompilation. These approaches, however, are unprincipled, requiring large engineering effort to maintain, and do not support symbolic dependencies, making them unsuitable for whole-program optimization and scheduling.

**Dynamic access patterns in DL** are common across various DL domains. Causal, sliding-window, anti-causal, blocked, and other patterns appear in attention-based models [90], flow networks [66], signal processing [91], time-series forecasting [92], temporal and video processing [93, 94], and RLHF [95]. By supporting dynamic dependencies through symbolic expressions, TIMERL has potential to efficiently optimize and manage more general DL computations.

## 10 Conclusion

We described TIMERL, a system that combines the flexibility of eager execution with the program-wide optimizations and scheduling of graph-based execution for DRL algorithms. From a recurrent tensor program, TIMERL constructs a polyhedral dependence graph that encodes dynamic dependencies as symbolic expressions, enabling optimizations such as vectorization, incrementalization, and fusion. TIMERL then computes an efficient execution schedule, including buffer deallocations, donations, and GPU/CPU memory swaps. TIMERL achieves substantial performance speed-ups, while tailoring execution to specific algorithms, demonstrating its potential for whole-program optimization and scheduling of dynamic DL programs.

## References

- [1] Richard S Sutton and Andrew G Barto. *Reinforcement learning: An introduction*. MIT press, 2018.
- [2] David Silver, Aja Huang, Chris J Maddison, Arthur Guez, Laurent Sifre, George Van Den Driessche, Julian Schrittwieser, Ioannis Antonoglou, Veda Panneershelvam, Marc Lanctot, et al. Mastering the game of go with deep neural networks and tree search. *nature*, 529(7587):484–489, 2016.
- [3] Oriol Vinyals, Igor Babuschkin, Wojciech M Czarnecki, Michaël Mathieu, Andrew Dudzik, Junyoung Chung, David H Choi, Richard Powell, Timo Ewalds, Petko Georgiev, et al. Grandmaster level in starcraft ii using multi-agent reinforcement learning. *Nature*, 575(7782):350–354, 2019.
- [4] Julian Schrittwieser, Ioannis Antonoglou, Thomas Hubert, Karen Simonyan, Laurent Sifre, Simon Schmitt, Arthur Guez, Edward Lockhart, Demis Hassabis, Thore Graepel, et al. Mastering atari, go, chess and shogi by planning with a learned model. *Nature*, 588(7839):604–609, 2020.
- [5] Shixiang Gu, Ethan Holly, Timothy Lillicrap, and Sergey Levine. Deep reinforcement learning for robotic manipulation with asynchronous off-policy updates. In *2017 IEEE international conference on robotics and automation (ICRA)*, pages 3389–3396. IEEE, 2017.
- [6] Tuomas Haarnoja, Sehoon Ha, Aurick Zhou, Jie Tan, George Tucker, and Sergey Levine. Learning to walk via deep reinforcement learning. *arXiv preprint arXiv:1812.11103*, 2018.
- [7] Alhussein Fawzi, Matej Balog, Aja Huang, Thomas Hubert, Bernardino Romera-Paredes, Mohammadamin Barekattain, Alexander Novikov, Francisco J R Ruiz, Julian Schrittwieser, Grzegorz Swirszcz, et al. Discovering faster matrix multiplication algorithms with reinforcement learning. *Nature*, 610(7930):47–53, 2022.
- [8] Daniel J Mankowitz, Andrea Michi, Anton Zhernov, Marco Gelmi, Marco Selvi, Cosmin Paduraru, Edouard Leurent, Shariq Iqbal, Jean-Baptiste Lespiau, Alex Ahern, et al. Faster sorting algorithms discovered using deep reinforcement learning. *Nature*, 618(7964):257–263, 2023.
- [9] Azalia Mirhoseini, Anna Goldie, Mustafa Yazgan, Joe Wenjie Jiang, Ebrahim Songhori, Shen Wang, Young-Joon Lee, Eric Johnson, Omkar Pathak, Azade Nazi, et al. A graph placement methodology for fast chip design. *Nature*, 594(7862):207–212, 2021.
- [10] Nisan Stiennon, Long Ouyang, Jeffrey Wu, Daniel Ziegler, Ryan Lowe, Chelsea Voss, Alec Radford, Dario Amodei, and Paul F Christiano. Learning to summarize with human feedback. *Advances in Neural Information Processing Systems*, 33:3008–3021, 2020.
- [11] Long Ouyang, Jeffrey Wu, Xu Jiang, Diogo Almeida, Carroll Wainwright, Pamela Mishkin, Chong Zhang, Sandhini Agarwal, Katarina Slama, Alex Ray, et al. Training language models to follow instructions with human feedback. *Advances in neural information processing systems*, 35:27730–27744, 2022.
- [12] Barret Zoph and Quoc V. Le. Neural architecture search with reinforcement learning. *CoRR*, abs/1611.01578, 2016.
- [13] Lisha Li, Kevin Jamieson, Giulia DeSalvo, Afshin Roshtamizadeh, and Ameet Talwalkar. Hyperband: A novel bandit-based approach to hyperparameter optimization. *Journal of Machine Learning Research*, 18(185):1–52, 2018.
- [14] Ekin D Cubuk, Barret Zoph, Dandelion Mane, Vijay Vasudevan, and Quoc V Le. Autoaugment: Learning augmentation policies from data. *arXiv preprint arXiv:1805.09501*, 2018.
- [15] Greg Brockman, Vicki Cheung, Ludwig Pettersson, Jonas Schneider, John Schulman, Jie Tang, and Wojciech Zaremba. Openai gym. *arXiv preprint arXiv:1606.01540*, 2016.
- [16] Ronald J Williams. Simple statistical gradient-following algorithms for connectionist reinforcement learning. *Machine learning*, 8(3):229–256, 1992.
- [17] John Schulman, F. Wolski, Prafulla Dhariwal, Alec Radford, and Oleg Klimov. Proximal policy optimization algorithms. *ArXiv*, abs/1707.06347, 2017.
- [18] Gavin A Rummery and Mahesan Nirranjan. *On-line Q-learning using connectionist systems*, volume 37. Cite-seer, 1994.
- [19] Richard S Sutton. Learning to predict by the methods of temporal differences. *Machine learning*, 3(1):9–44, 1988.
- [20] Yanping Huang, Youlong Cheng, Ankur Bapna, Orhan Firat, Dehao Chen, Mia Chen, HyoukJoong Lee, Jiquan Ngiam, Quoc V Le, Yonghui Wu, et al. Gpipe: Efficient training of giant neural networks using pipeline parallelism. *Advances in neural information processing systems*, 32, 2019.
- [21] Minsoo Rhu, Natalia Gimelshein, Jason Clemons, Arslan Zulfiqar, and Stephen W Keckler. vdn: Virtualized

- deep neural networks for scalable, memory-efficient neural network design. In *2016 49th Annual IEEE/ACM International Symposium on Microarchitecture (MICRO)*, pages 1–13. IEEE, 2016.
- [22] Jack J Dongarra, Jeremy Du Croz, Sven Hammarling, and Richard J Hanson. An extended set of fortran basic linear algebra subprograms. *ACM Trans. Math. Softw.*, 14(1):1–17, 1988.
- [23] Volodymyr Mnih, Adria Puigdomenech Badia, Mehdi Mirza, Alex Graves, Timothy Lillicrap, Tim Harley, David Silver, and Koray Kavukcuoglu. Asynchronous methods for deep reinforcement learning. In *International conference on machine learning*, pages 1928–1937. PMLR, 2016.
- [24] Adam Paszke, Sam Gross, Francisco Massa, Adam Lerer, James Bradbury, Gregory Chanan, Trevor Killeen, Zeming Lin, Natalia Gimelshein, Luca Antiga, et al. Pytorch: An imperative style, high-performance deep learning library. *Advances in neural information processing systems*, 32, 2019.
- [25] Martín Abadi, P. Barham, J. Chen, Z. Chen, Andy Davis, J. Dean, M. Devin, Sanjay Ghemawat, Geoffrey Irving, M. Isard, M. Kudlur, Josh Levenberg, Rajat Monga, Sherry Moore, D. Murray, Benoit Steiner, P. Tucker, Vijay Vasudevan, Pete Warden, Martin Wicke, Y. Yu, and Xiaoqiang Zhang. Tensorflow: A system for large-scale machine learning. In *OSDI*, 2016.
- [26] Roy Frostig, Matthew James Johnson, and Chris Leary. Compiling machine learning programs via high-level tracing. *Systems for Machine Learning*, pages 23–24, 2018.
- [27] Akshay Agrawal, Akshay Modi, Alexandre Passos, Allen Lavoie, Ashish Agarwal, Asim Shankar, Igor Ganchev, Josh Levenberg, Mingsheng Hong, Rajat Monga, et al. Tensorflow eager: A multi-stage, python-embedded dsl for machine learning. *Proceedings of Machine Learning and Systems*, 1:178–189, 2019.
- [28] Yuan Yu, Martín Abadi, Paul Barham, Eugene Brevdo, Mike Burrows, Andy Davis, Jeff Dean, Sanjay Ghemawat, Tim Harley, Peter Hawkins, et al. Dynamic control flow in large-scale machine learning. In *Proceedings of the Thirteenth EuroSys Conference*, pages 1–15, 2018.
- [29] Matteo Hessel, Manuel Kroiss, Aidan Clark, Iurii Kemaev, John Quan, Thomas Keck, Fabio Viola, and Hado van Hasselt. Podracer architectures for scalable reinforcement learning. *arXiv preprint arXiv:2104.06272*, 2021.
- [30] Eric Liang, Richard Liaw, Robert Nishihara, Philipp Moritz, Roy Fox, Ken Goldberg, Joseph Gonzalez, Michael Jordan, and Ion Stoica. Rllib: Abstractions for distributed reinforcement learning. In *International Conference on Machine Learning*, pages 3053–3062. PMLR, 2018.
- [31] Shengyi Huang, Rousslan Fernand Julien Dossa, Chang Ye, Jeff Braga, Dipam Chakraborty, Kinal Mehta, and João GM Araújo. Cleanrl: High-quality single-file implementations of deep reinforcement learning algorithms. *Journal of Machine Learning Research*, 23(274):1–18, 2022.
- [32] Aleksei Petrenko, Zhehui Huang, T. Kumar, G. Sukhatme, and V. Koltun. Sample factory: Egocentric 3d control from pixels at 100000 fps with asynchronous reinforcement learning. *ArXiv*, abs/2006.11751, 2020.
- [33] A. Inci, E. Bolotin, Yaosheng Fu, Gal Dalal, Shie Mannor, David W. Nellans, and Diana Marculescu. The architectural implications of distributed reinforcement learning on cpu-gpu systems. *ArXiv*, abs/2012.04210, 2020.
- [34] James Gleeson, Srivatsan Krishnan, Moshe Gabel, Vijay Janapa Reddi, Eyal de Lara, and Gennady Pekhimenko. RL-Scope: cross-stack profiling for deep reinforcement learning workloads. In *Proceedings of Machine Learning and Systems*, 2021.
- [35] Richard M Karp, Raymond E Miller, and Shmuel Winograd. The organization of computations for uniform recurrence equations. *Journal of the ACM (JACM)*, 14(3):563–590, 1967.
- [36] Sven Verdoolaege. isl: An integer set library for the polyhedral model. In *International Congress on Mathematical Software*, pages 299–302. Springer, 2010.
- [37] Uday Bondhugula, Albert Hartono, J Ramanujam, and P Sadayappan. Pluto: A practical and fully automatic polyhedral program optimization system. In *Proceedings of the ACM SIGPLAN 2008 Conference on Programming Language Design and Implementation (PLDI 08)*, Tucson, AZ (June 2008). Citeseer, 2008.
- [38] Adam Stooke and Pieter Abbeel. Accelerated methods for deep reinforcement learning. *arXiv preprint arXiv:1803.02811*, 2018.
- [39] Sam McCandlish, Jared Kaplan, Dario Amodei, and OpenAI Dota Team. An empirical model of large-batch training. *arXiv preprint arXiv:1812.06162*, 2018.

- [40] C Daniel Freeman, Erik Frey, Anton Raichuk, Sertan Girgin, Igor Mordatch, and Olivier Bachem. Brax—a differentiable physics engine for large scale rigid body simulation. *arXiv preprint arXiv:2106.13281*, 2021.
- [41] Lasse Espeholt, Raphaël Marinier, P. Stanczyk, Ke Wang, and Marcin Michalski. Seed rl: Scalable and efficient deep-rl with accelerated central inference. *ArXiv*, abs/1910.06591, 2020.
- [42] Lasse Espeholt, Hubert Soyer, Remi Munos, Karen Simonyan, Vlad Mnih, Tom Ward, Yotam Doron, Vlad Firoiu, Tim Harley, Iain Dunning, et al. Impala: Scalable distributed deep-rl with importance weighted actor-learner architectures. In *International Conference on Machine Learning*, pages 1407–1416. PMLR, 2018.
- [43] Heinrich Küttler, Nantas Nardelli, Thibaut Lavril, Marco Selvatici, Viswanath Sivakumar, Tim Rocktäschel, and Edward Grefenstette. Torchbeast: A pytorch platform for distributed rl. *arXiv preprint arXiv:1910.03552*, 2019.
- [44] Steven Dalton and I. Frosio. Accelerating reinforcement learning through gpu atari emulation. *arXiv: Learning*, 2020.
- [45] Viktor Makoviychuk, Lukasz Wawrzyniak, Yunrong Guo, Michelle Lu, Kier Storey, Miles Macklin, David Hoeller, Nikita Rudin, Arthur Allshire, Ankur Handa, et al. Isaac gym: High performance gpu-based physics simulation for robot learning. *arXiv preprint arXiv:2108.10470*, 2021.
- [46] Brennan Shacklett, Erik Wijmans, Aleksei Petrenko, M. Savva, Dhruv Batra, V. Koltun, and K. Fatahalian. Large batch simulation for deep reinforcement learning. *ArXiv*, abs/2103.07013, 2021.
- [47] Jiayi Weng, Min Lin, Shengyi Huang, Bo Liu, Denys Makoviichuk, Viktor Makoviychuk, Zichen Liu, Yufan Song, Ting Luo, Yukun Jiang, et al. Envpool: A highly parallel reinforcement learning environment execution engine. *arXiv preprint arXiv:2206.10558*, 2022.
- [48] Volodymyr Mnih, Koray Kavukcuoglu, David Silver, Alex Graves, Ioannis Antonoglou, Daan Wierstra, and Martin Riedmiller. Playing atari with deep reinforcement learning. *arXiv preprint arXiv:1312.5602*, 2013.
- [49] Lili Chen, Kevin Lu, Aravind Rajeswaran, Kimin Lee, Aditya Grover, Misha Laskin, Pieter Abbeel, Aravind Srinivas, and Igor Mordatch. Decision transformer: Reinforcement learning via sequence modeling. *Advances in neural information processing systems*, 34:15084–15097, 2021.
- [50] Tuomas Haarnoja, Aurick Zhou, Pieter Abbeel, and Sergey Levine. Soft actor-critic: Off-policy maximum entropy deep reinforcement learning with a stochastic actor. In *International conference on machine learning*, pages 1861–1870. PMLR, 2018.
- [51] Paul J Werbos. Backpropagation through time: what it does and how to do it. *Proceedings of the IEEE*, 78(10):1550–1560, 1990.
- [52] Alex Suhan, Davide Libenzi, Ailing Zhang, Parker Schuh, Brennan Saeta, Jie Young Sohn, and Denys Shabalin. Lazytensor: combining eager execution with domain-specific compilers. *arXiv preprint arXiv:2102.13267*, 2021.
- [53] Operation semantics | xla | tensorflow.
- [54] Jason Ansel, Edward Yang, Horace He, Natalia Gimelshein, Animesh Jain, Michael Voznesensky, Bin Bao, Peter Bell, David Berard, Evgeni Burovski, et al. Pytorch 2: Faster machine learning through dynamic python bytecode transformation and graph compilation. In *Proceedings of the 29th ACM International Conference on Architectural Support for Programming Languages and Operating Systems, Volume 2*, pages 929–947, 2024.
- [55] Adam Stooke and Pieter Abbeel. rlypt: A research code base for deep reinforcement learning in pytorch. *arXiv preprint arXiv:1909.01500*, 2019.
- [56] Matt Hoffman, Bobak Shahriari, John Aslanides, Gabriel Barth-Maron, Feryal Behbahani, Tamara Norman, Abbas Abdolmaleki, Albin Cassirer, Fan Yang, Kate Baumli, et al. Acme: A research framework for distributed reinforcement learning. *arXiv preprint arXiv:2006.00979*, 2020.
- [57] Jiayi Weng, Huayu Chen, Dong Yan, Kaichao You, Alexis Duburcq, Minghao Zhang, Hang Su, and Jun Zhu. Tianshou: A highly modularized deep reinforcement learning library. *arXiv preprint arXiv:2107.14171*, 2021.
- [58] Denys Makoviichuk and Viktor Makoviychuk. rl-games: A high-performance framework for reinforcement learning. [https://github.com/Denys88/rl\\_games](https://github.com/Denys88/rl_games), May 2022.
- [59] Albert Bou, Matteo Bettini, Sebastian Dittert, Vikash Kumar, Shagun Sodhani, Xiaomeng Yang, Gianni De Fabritiis, and Vincent Moens. Torchrl: A data-driven decision-making library for pytorch. *arXiv preprint arXiv:2306.00577*, 2023.

- [60] Christopher Berner, Greg Brockman, Brooke Chan, Vicki Cheung, Przemysław Dębniak, Christy Dennison, David Farhi, Quirin Fischer, Shariq Hashme, Chris Hesse, et al. Dota 2 with large scale deep reinforcement learning. *arXiv preprint arXiv:1912.06680*, 2019.
- [61] Atilim Gunes Baydin, Barak A Pearlmutter, Alexey Andreyevich Radul, and Jeffrey Mark Siskind. Automatic differentiation in machine learning: a survey. *Journal of Machine Learning Research*, 18:1–43, 2018.
- [62] Inc. DMLC. Dlpack: Open in-memory tensor structure. <https://github.com/dmlc/dlpack>. Accessed: 2024-11-07.
- [63] Yusuke Fujii, Takuya Azumi, Nobuhiko Nishio, Shinpei Kato, and Masato Eda. Data transfer matters for gpu computing. In *2013 International Conference on Parallel and Distributed Systems*, pages 275–282. IEEE, 2013.
- [64] Diederik P Kingma and Jimmy Ba. Adam: A method for stochastic optimization. *arXiv preprint arXiv:1412.6980*, 2014.
- [65] Christian Darken and John Moody. Note on learning rate schedules for stochastic optimization. *Advances in neural information processing systems*, 3, 1990.
- [66] Emmanuel Bengio, Moksh Jain, Maksym Korablyov, Doina Precup, and Yoshua Bengio. Flow network based generative models for non-iterative diverse candidate generation. *Advances in Neural Information Processing Systems*, 34:27381–27394, 2021.
- [67] Jonathan Ho, Ajay Jain, and Pieter Abbeel. Denoising diffusion probabilistic models. *Advances in neural information processing systems*, 33:6840–6851, 2020.
- [68] John Schulman, Philipp Moritz, Sergey Levine, Michael Jordan, and Pieter Abbeel. High-dimensional continuous control using generalized advantage estimation. *arXiv preprint arXiv:1506.02438*, 2015.
- [69] Albin Cassirer, Gabriel Barth-Maron, Eugene Brevdo, Sabela Ramos, Toby Boyd, Thibault Sottiaux, and Manuel Kroiss. Reverb: a framework for experience replay. *arXiv preprint arXiv:2102.04736*, 2021.
- [70] Tom Schaul, John Quan, Ioannis Antonoglou, and David Silver. Prioritized experience replay. *arXiv preprint arXiv:1511.05952*, 2015.
- [71] Philippe Tillet, Hsiang-Tsung Kung, and David Cox. Triton: an intermediate language and compiler for tiled neural network computations. In *Proceedings of the 3rd ACM SIGPLAN International Workshop on Machine Learning and Programming Languages*, pages 10–19, 2019.
- [72] Mohamed-Walid Benabderrahmane, Louis-Noël Pouchet, Albert Cohen, and Cédric Bastoul. The polyhedral model is more widely applicable than you think. In *International Conference on Compiler Construction*, pages 283–303. Springer, 2010.
- [73] Tobias Grosser, Armin Groesslinger, and Christian Lengauer. Polly—performing polyhedral optimizations on a low-level intermediate representation. *Parallel Processing Letters*, 22(04):1250010, 2012.
- [74] Nicolas Vasilache, Oleksandr Zinenko, Theodoros Theodoridis, Priya Goyal, Zachary DeVito, William S Moses, Sven Verdoolaege, Andrew Adams, and Albert Cohen. Tensor comprehensions: Framework-agnostic high-performance machine learning abstractions. *arXiv preprint arXiv:1802.04730*, 2018.
- [75] Sven Verdoolaege and Tobias Grosser. Polyhedral extraction tool. In *Second International Workshop on Polyhedral Compilation Techniques (IMPACT’12), Paris, France*, volume 141, 2012.
- [76] Christoph Haase. A survival guide to presburger arithmetic. *ACM SIGLOG News*, 5(3):67–82, 2018.
- [77] Tobias Grosser, Sven Verdoolaege, and Albert Cohen. Polyhedral ast generation is more than scanning polyhedra. *ACM Transactions on Programming Languages and Systems (TOPLAS)*, 37(4):1–50, 2015.
- [78] NVIDIA Corporation. Getting started with cuda graphs, 2020. Accessed: 2024-12-07.
- [79] Ankur Handa, Arthur Allshire, Viktor Makoviychuk, Aleksei Petrenko, Ritvik Singh, Jingzhou Liu, Denys Makoviichuk, Karl Van Wyk, Alexander Zhurkevich, Balakumar Sundaralingam, et al. Dextreme: Transfer of agile in-hand manipulation from simulation to reality. In *2023 IEEE International Conference on Robotics and Automation (ICRA)*, pages 5977–5984. IEEE, 2023.
- [80] B Ravi Kiran, Ibrahim Sobh, Victor Talpaert, Patrick Mannion, Ahmad A Al Sallab, Senthil Yogamani, and Patrick Pérez. Deep reinforcement learning for autonomous driving: A survey. *IEEE Transactions on Intelligent Transportation Systems*, 23(6):4909–4926, 2021.
- [81] Chao Yu, Jiming Liu, Shamim Nemati, and Guosheng Yin. Reinforcement learning in healthcare: A survey. *ACM Computing Surveys (CSUR)*, 55(1):1–36, 2021.
- [82] Sven Verdoolaege, Juan Carlos Juega, Albert Cohen, Jose Ignacio Gomez, Christian Tenllado, and Francky Catthoor. Polyhedral parallel code generation for cuda. *ACM Transactions on Architecture and Code Optimization (TACO)*, 9(4):1–23, 2013.



- [83] Tianqi Chen, Thierry Moreau, Ziheng Jiang, Lianmin Zheng, Eddie Yan, Haichen Shen, Meghan Cowan, Leyuan Wang, Yuwei Hu, Luis Ceze, et al. {TVM}: An automated {End-to-End} optimizing compiler for deep learning. In *13th USENIX Symposium on Operating Systems Design and Implementation (OSDI 18)*, pages 578–594, 2018.
- [84] Shixiong Zhao, Fanxin Li, Xusheng Chen, Xiuxian Guan, Jianyu Jiang, Dong Huang, Yuhao Qing, Sen Wang, Peng Wang, Gong Zhang, et al. v pipe: A virtualized acceleration system for achieving efficient and scalable pipeline parallel dnn training. *IEEE Transactions on Parallel and Distributed Systems*, 33(3):489–506, 2021.
- [85] Chien-Chin Huang, Gu Jin, and Jinyang Li. Swapadvisor: Pushing deep learning beyond the gpu memory limit via smart swapping. In *Proceedings of the Twenty-Fifth International Conference on Architectural Support for Programming Languages and Operating Systems*, pages 1341–1355, 2020.
- [86] Linnan Wang, Jinmian Ye, Yiyang Zhao, Wei Wu, Ang Li, Shuaiwen Leon Song, Zenglin Xu, and Tim Kraska. Superneurons: Dynamic gpu memory management for training deep neural networks. In *Proceedings of the 23rd ACM SIGPLAN symposium on principles and practice of parallel programming*, pages 41–53, 2018.
- [87] Xuan Peng, Xuanhua Shi, Hulin Dai, Hai Jin, Weiliang Ma, Qian Xiong, Fan Yang, and Xuehai Qian. Capuchin: Tensor-based gpu memory management for deep learning. In *Proceedings of the Twenty-Fifth International Conference on Architectural Support for Programming Languages and Operating Systems*, pages 891–905, 2020.
- [88] Siran Liu, Chengxiang Qi, Ying Cao, Chao Yang, Weifang Hu, Xuanhua Shi, Fan Yang, and Mao Yang. Uncovering nested data parallelism and data reuse in dnn computation with fractaltensor. In *SOSP*, November 2024.
- [89] Eunji Jeong, Sungwoo Cho, Gyeong-In Yu, Joo Seong Jeong, Dong-Jin Shin, Taebum Kim, and Byung-Gon Chun. Speculative symbolic graph execution of imperative deep learning programs. *ACM SIGOPS Operating Systems Review*, 53(1):26–33, 2019.
- [90] Ashish Vaswani, Noam Shazeer, Niki Parmar, Jakob Uszkoreit, Llion Jones, Aidan N. Gomez, Lukasz Kaiser, and Illia Polosukhin. Attention is all you need. In *Proceedings of the 31st International Conference on Neural Information Processing Systems, NIPS’17*, page 6000–6010, Red Hook, NY, USA, 2017. Curran Associates Inc.
- [91] Alan V Oppenheim, Alan S Willsky, Syed Hamid Nawab, and Jian-Jiun Ding. *Signals and systems*, volume 2. Prentice hall Upper Saddle River, NJ, 1997.
- [92] Bryan Lim and Stefan Zohren. Time-series forecasting with deep learning: a survey. *Philosophical Transactions of the Royal Society A*, 379(2194):20200209, 2021.
- [93] Colin Lea, Michael D Flynn, Rene Vidal, Austin Reiter, and Gregory D Hager. Temporal convolutional networks for action segmentation and detection. In *proceedings of the IEEE Conference on Computer Vision and Pattern Recognition*, pages 156–165, 2017.
- [94] Xuezhe Ma, Chunting Zhou, Xiang Kong, Junxian He, Liangke Gui, Graham Neubig, Jonathan May, and Luke Zettlemoyer. Mega: moving average equipped gated attention. *arXiv preprint arXiv:2209.10655*, 2022.
- [95] Paul F Christiano, Jan Leike, Tom Brown, Miljan Martic, Shane Legg, and Dario Amodei. Deep reinforcement learning from human preferences. *Advances in neural information processing systems*, 30, 2017.